

Systematic climate model biases in the large-scale pattern of sea-surface temperature and sea-level pressure change

Robert Jnglin Wills¹, Yue Dong², Cristian Proistosescu³, Kyle Armour¹, David Battisti¹

¹University of Washington, ²Lamont-Doherty Earth Observatory, ³University of Illinois – Correspondence: rcwills@uw.edu

Key Points

- Observed sea-surface temperature and sea-level pressure trends (1979-2020) are endmembers of what can be simulated by climate model large ensembles in many regions and indices
- The relative warm pool warming rate, which is important for climate sensitivity (Dong et al. 2019) and not thought to be strongly influenced by multi-decadal variability (Wills et al. 2021), is particularly anomalous
- A signal-to-noise maximizing pattern analysis is used to isolate changes that occurred in observations that models are unable to reproduce

How anomalous are observed trends?

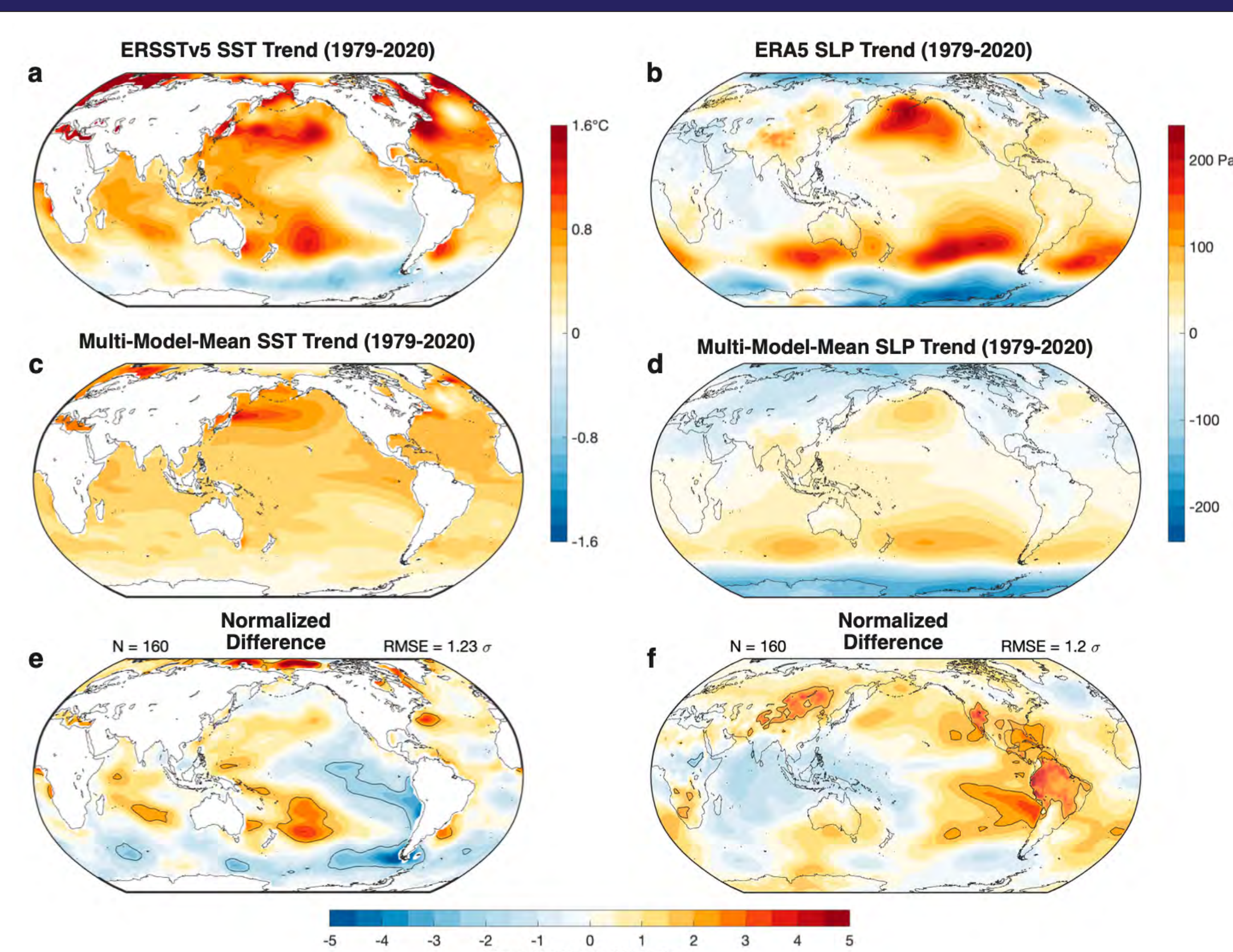


Figure 1. Observed trends in annual-mean (a) SST and (b) SLP over 1979–2020 from ERSSTv5 (Huang et al., 2017) and the ERA5 reanalysis (Hersbach et al., 2020), respectively. Modeled trends in (c) SST and (d) SLP over 1979–2020, from the multi-model ensemble mean of historical simulations with 16 climate model LEs (Table 1). The SST trends in each simulation have been rescaled such that their global mean matches that in ERSSTv5. Observed trends in (e) SST and (f) SLP over 1979–2020 expressed in ensemble standard deviations away from the multi-model ensemble mean (i.e., the difference in trends between observations and the multi-model ensemble mean divided by the square root of the multi-model mean of the variance in trends within each large ensemble). Panels (c)–(f) are computed with the first 10 members of each large ensemble such that each model is weighted equally. The ± 2 standard deviation contour is shown with a black line.

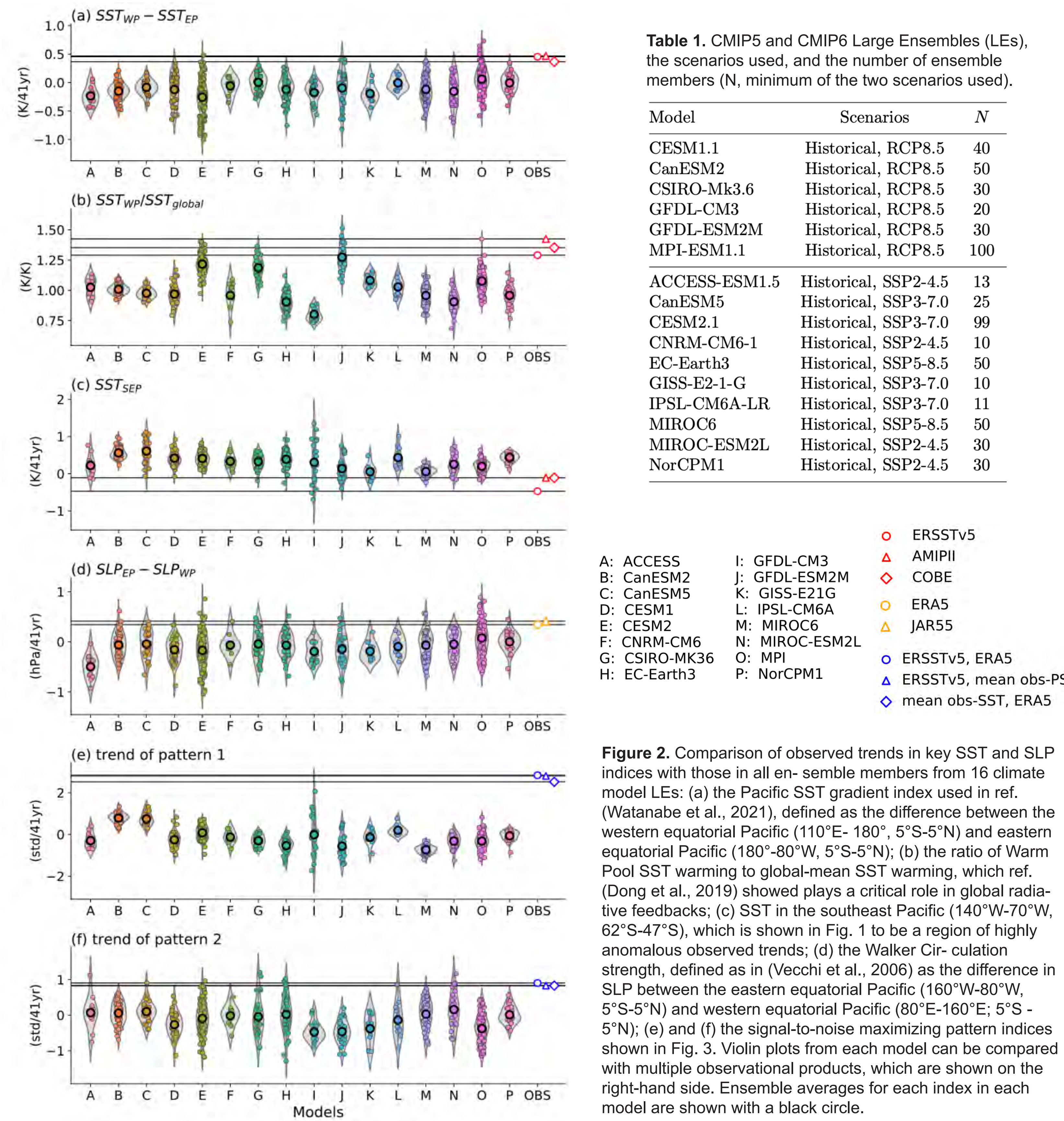


Table 1. CMIP5 and CMIP6 Large Ensembles (LEs), the scenarios used, and the number of ensemble members (N, minimum of the two scenarios used).

Model	Scenarios	N
CESM1.1	Historical, RCP8.5	40
CanESM2	Historical, RCP8.5	50
CSIRO-Mk3.6	Historical, RCP8.5	30
GFDL-CM3	Historical, RCP8.5	20
GFDL-ESM2M	Historical, RCP8.5	30
MPI-ESM1.1	Historical, RCP8.5	100
ACCESS-ESM1.5	Historical, SSP2-4.5	13
CanESM5	Historical, SSP3-7.0	25
CESM2.1	Historical, SSP3-7.0	99
CNRM-CM6-1	Historical, SSP2-4.5	10
EC-Earth3	Historical, SSP5-8.5	50
GISS-E2-1-G	Historical, SSP3-7.0	10
IPSL-CM6A-LR	Historical, SSP3-7.0	11
MIROC6	Historical, SSP5-8.5	50
MIROC-ESM2L	Historical, SSP2-4.5	30
NorCPM1	Historical, SSP2-4.5	30

A: ACCESS
B: CanESM2
C: CanESM5
D: CESM1
E: CESM2
F: CNRM-CM6
G: CSIRO-Mk3.6
H: EC-Earth3
I: GFDL-CM3
J: GFDL-ESM2M
K: GISS-E2.1G
L: IPSL-CM6A
M: MIROC6
N: MIROC-ESM2L
O: MPI
P: NorCPM1

○ ERSSTv5
△ AMIPII
◇ COBE
○ ERA5
△ JAR55
○ ERSSTv5, ERA5
△ ERSSTv5, mean obs-PSL
◇ mean obs-SST, ERA5

Figure 2. Comparison of observed trends in key SST and SLP indices with those in all ensemble members from 16 climate model LEs: (a) the Pacific SST gradient index used in ref. (Watanabe et al., 2021), defined as the difference between the western equatorial Pacific (110°E–180°, 5°S–5°N) and eastern equatorial Pacific (180°–80°W, 5°S–5°N); (b) the ratio of Warm Pool SST warming to global-mean SST warming, which ref. (Dong et al., 2019) showed plays a critical role in global radiative feedbacks; (c) SST in the southeast Pacific (140°W–70°W, 62°S–47°S), which is shown in Fig. 1 to be a region of highly anomalous observed trends; (d) the Walker Circulation strength, defined as in (Vecchi et al., 2006) as the difference in SLP between the eastern equatorial Pacific (160°W–80°W, 5°S–5°N) and western equatorial Pacific (80°E–160°E; 5°S–5°N); (e) and (f) the signal-to-noise maximizing pattern indices shown in Fig. 3. Violin plots from each model can be compared with multiple observational products, which are shown on the right-hand side. Ensemble averages for each index in each model are shown with a black circle.

Patterns found in OBS but not models

- Here, we set up a signal-to-noise maximizing analysis (Venzke et al. 1999; Schneider & Griffies 1999; Ting et al. 2009; Wills et al. 2020) to find a pattern of change that is most anomalous in observations relative to modeled variability and change (basically weighting the regions with large values in Fig. 1e/f, but putting this back into real units of °C and Pa).
- To do this, we make an ensemble where each member is observations minus one of the 160 ensemble members (16 models x 10 members each). We then solve for the pattern that has the largest fraction of variance in the ensemble mean (i.e., observations - ensemble mean) and thus the smallest fraction of variance explained by inter-ensemble member variations (including inter-model differences).
- The resulting patterns and timeseries show the amplitude of anomalies (from the multi-model ensemble mean) in observations (orange/black) and models (grey).

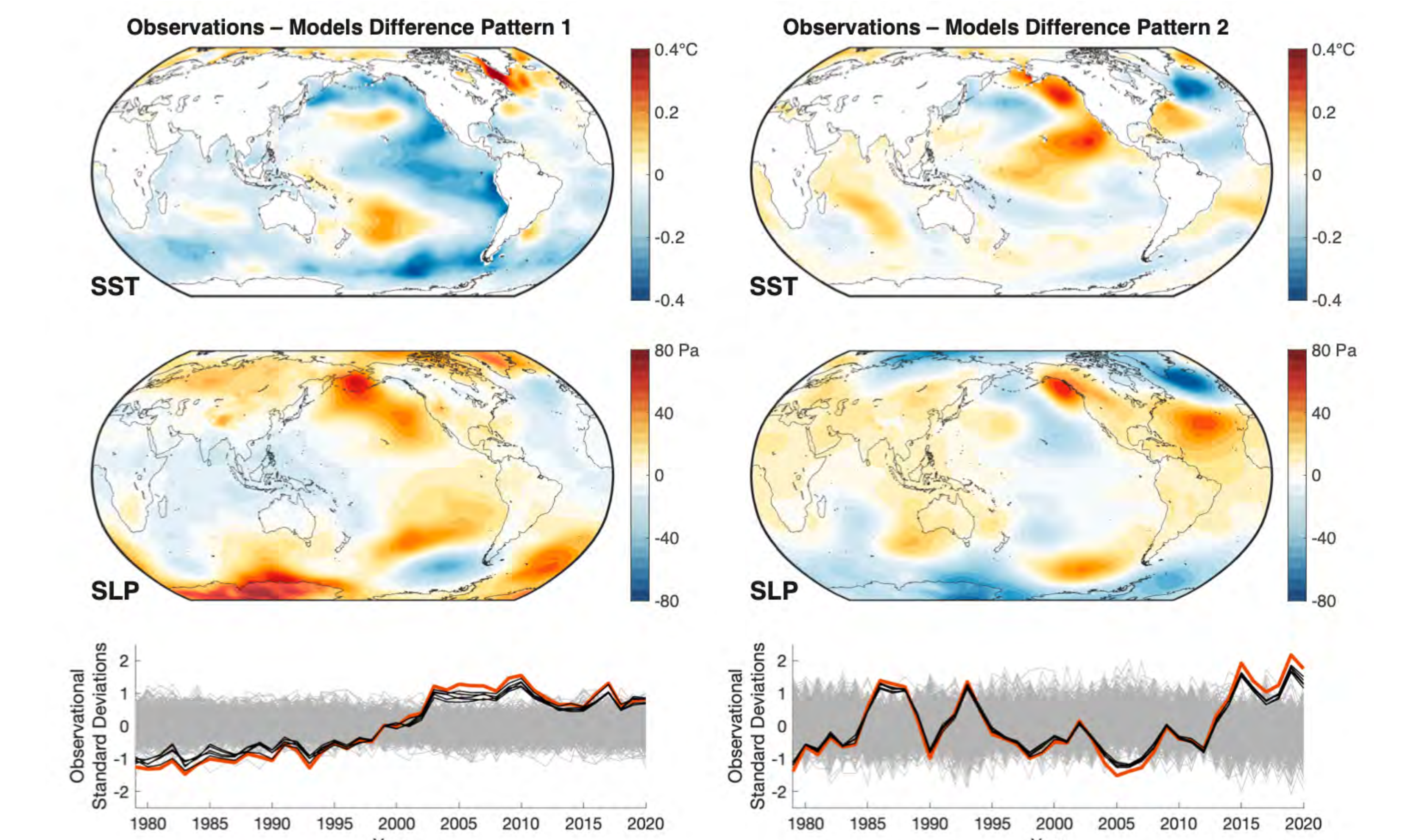


Figure 3. First and second multi-field (SST and SLP) signal-to-noise maximizing patterns, from a signal-to-noise maximizing pattern analysis that maximizes the ratio of signal to noise, where signal is defined as the difference between observations and the multi-model ensemble mean and noise is defined as intra-model and inter-model differences. The orange timeseries show the amplitude of anomalies in these pattern in ERSSTv5/ERA5 relative to the multi-model ensemble mean and the black lines show the amplitude of anomalies in these pattern in the other 4 combinations of SST and SLP observational products. The grey lines show the amplitude of these patterns in each of the 598 simulations from the multi-model ensemble. Normalization is such that the orange line has unit standard deviation and the SST/SLP pattern shows the anomalies associated with a 1-standard-deviation anomaly in the associated index.

Possible Explanations, Open Questions

Possible explanations for trend discrepancy between models and observations:

- The relative warming of the warm pool index (Fig. 2b) has limited multi-decadal variability, because there are strong global radiative feedbacks in response to warming in this region (Dong et al. 2019; Wills et al. 2021). We think this indicates a forced response bias (in the 12 models that can't reproduce observed trends), potentially related to a too-strong global feedback in response to warming in this region (e.g., a problem with deep convection parameterization).
- Reducing the global feedback for warm pool warming could also lead to more multi-decadal variability in this region, as is suggested by proxies (Laepple and Huybers 2014)
- Likely a contribution to the trend discrepancy from biases in Southern Ocean trends, e.g., from biases in the westerly wind response to forcing, from missing Antarctic meltwater forcing, or from Southern Ocean multi-decadal variability. Notably, forcing CESM1 with observed winds over 40–80°S shows closer to observed trends (Armour et al., in prep).
- Biases in the tropical Pacific climatological SST, wind, and relative humidity can lead to biases in forced SST trends (Seager et al. 2019).
- Models with better representation of ENSO nonlinearity (e.g., GFDL-ESM2M) may better reproduce observed trends in the tropics (Kohyama et al. 2017; Karamperidou et al. 2017)

Open questions:

- Is the global feedback for warm pool warming too large in models? (GF-MIP)
- What are the relative contributions of forced response and internal variability to the patterns in Figure 3?
- When will the East Pacific & Southern Ocean warming expected in equilibrium emerge?

Conclusions and Implications

- Models have biases in their forced SST and SLP response, have too little multi-decadal variability, or a combination of both
- The observed warming pattern favors low cloud increases in the eastern Pacific that bias estimates of ECS based on observations low (assuming East Pacific and Southern Ocean warm eventually) (Armour, Proistosescu et al. in prep.)
- If the observed SST trend is a transient forced response and models have the correct equilibrium SST pattern, this implies a larger pattern effect in the real world than models

Wills, R.C.J., Y. Dong, C. Proistosescu, K.C. Armour, and D.S. Battisti, 2022: **Systematic climate model biases in the large-scale pattern of sea-surface temperature and sea-level pressure change**, will be submitted to Geophysical Research Letters by the end of this month and posted on atmos.washington.edu/~rcwills/publications/. (all other references can be found therein)